PNAS
www.pnas.org

Supplementary Information for

TRPV4-mediated Calcium Signaling in Mesenchymal Stem Cells Regulates Aligned Collagen Matrix Formation and Vinculin Tension

Christopher L. Gilchrist, Holly A. Leddy, Laurel Kaye, Natasha Case, Katheryn E. Rothenberg, Dianne Little, Wolfgang Liedtke, Brenton D. Hoffman, Farshid Guilak

Farshid Guilak, Ph.D.
Email: guilak@wustl.edu

Brenton D. Hoffman, Ph.D.
Email: brenton.hoffman@duke.edu

This PDF file includes:

Supplementary text
Figures S1 to S3
Captions for movies S1
References for SI reference citations

Other supplementary materials for this manuscript include the following:

Movie S1

www.pnas.org/cgi/doi/10.1073/pnas.1811095116

Supplementary Information Text

Supplementary Methods

Cell Culture. Human mesenchymal stem cells (MSCs) isolated from bone marrow aspirates (cells pooled from 3 de-identified donors, surgical waste approved as exempt from review by Duke University Institutional Review Board) were expanded in monolayer (passage 5) and seeded onto μPP substrates (25,000 cells/cm^2, unattached cells removed via media wash), and cultured (5% CO_2, 37°C) for 1-14 days on patterns in culture media (Advanced DMEM, Gibco/Life Technologies) with 10% FBS, 200 μM L-ascorbic acid 2-phosphate, 2 mM L-glutamine, and 1% penicillin-streptomycin).

Micro-Photopatterning (μPP). Cell-adhesive patterns with micro-scale architecture and macro-scale boundaries (Figs. 2A, S1A) were created via two-photon photoablation of thin (~150 nm) polyvinyl alcohol hydrogel layers (1, 2). Ablated cell-adhesive regions were functionalized with fibronectin (20 μg/ml) via adsorption. Two micro-scale μPP architectures were investigated: *Patterned* (2.0 μm-wide parallel lines spaced 5 μm on center), and *Unpatterned* (fully-ablated, no micro-scale pattern architecture), with varied macro-scale boundaries (Figs. 2A, S1A). Patterns are stable in culture for over 2 weeks.

TRPV4 Expression. TRPV4 protein expression in MSCs was assessed via immunostaining, western blot analysis, and flow cytometry using a TRPV4-specific antibody (ACC-034, Alamone Labs) (3). Articular chondrocytes, known to highly express TRPV4 (4), were isolated from young porcine femoral condyle cartilage and used as a positive control. Actin expression (I-19, Santa Cruz) was assessed to confirm equal protein loading between samples, and expression of the transcription factor Sox9 (H-90, Santa Cruz) was also evaluated for comparison between cell types. For immunofluorescent analyses, MSCs were fixed (4% formaldehyde), permeabilized (0.25% Triton X-100), stained with anti-TRPV4 primary and fluorescent secondary antibodies (Alexa Fluor 568, Thermo Fisher), and imaged (Zeiss LSM 510, 40X, 0.95NA). Samples stained without primary antibody were used as a negative control. Flow cytometric analyses were performed by detaching MSCs from their culture surface (0.05% trypsin/EDTA), fixing (4% formaldehyde), permeabilizing (0.1% saponin in PBS containing 5% goat serum) and labeling with anti-TRPV4 antibody (1:100 in PBS containing 1% BSA and 0.1% saponin; diluent only added for negative control) followed by fluorescent secondary antibody (Alexa Fluor 488, ThermoFisher Scientific). Labeled cell suspensions (n = 4, with 3 replicates/sample) were analyzed via flow cytometry (Accuri C6 flow cytometer), with the intensity threshold for positive expression set to exclude 99.5% of the negative control sample.

Polarized Light Analysis. Fibrillar collagen deposition was assessed using polarized light. Samples were fixed (4% formaldehyde, EMS, Hatfield, PA), stained with picrosirius red (ScyTek Labs, Logan, UT) to enhance fibrillar collagen birefringence, and imaged using a polarized light microscope (Olympus E600, 10X) equipped with rotating polarizer/analyzer (images acquired at 10° increments; mean pixel intensity over entire μPP pattern area measured for each sample using FIJI (NIH)). To detect differences between culture conditions, mean pattern intensities at a given polarizer angle were compared via ANOVA. The effects of TRPV4 inhibition and stimulation on fibrillar collagen deposition were also evaluated. For inhibition, MSCs on μPPs were cultured continuously with GSK205 (10 or 50 μM) or alternate TRPV4 inhibitors, HC067047 (10 μM, Tocris Bioscience, Bristol, UK) and RN1734 (10 μM, Sigma-Aldrich) for 14 days and analyzed via polarized light as described above. For activation experiments, MSCs on μPPs were treated with GSK101 (1 or 10 nM, or DMSO control) for 30 min/day (in culture media) for 7 or 14 days, and analyzed via polarized light.

Vinculin Tension Sensor Experiments. MSCs were transduced with lentivirus encoding a FRET-based intracellular biosensor designed to measure force across the focal adhesion protein vinculin (5), using transduction methods as previously described (6). The vinculin tension sensor (VinTS, Fig. 5A) consists of a tension sensor module (TSMod, with the FRET pair mTFP and Venus separated by a $[GGSGGS]_9$ linker sequence) inserted between the head and tail domains of vinculin. A mutant version of the sensor that fails to bind actin (VinTS I997A,(7)) was used as an actin-generated force insensitive control. Following transduction, MSCs were sorted via flow cytometry to select a uniform sensor expression level (based on mTFP fluorescence) and expanded to passage 5. To assess the role of TRPV4 in controlling force across vinculin, VinTS MSCs were seeded in a semi-confluent monolayer on FN-coated (10 μg/mL in PBS for 1h) glass coverslips and cultured for 3 days in the presence or absence of the TRPV4 inhibitor GSK205 (10 μM, 50 μM, or DMSO control). Treated VinTS MSCs were fixed (4% formaldehyde, 10 min) and imaged (Olympus UPlanSApo 60X/NA1.35 objective) using epi-fluorescent microscopy (Olympus IX83 equipped with a custom filter set for FRET imaging (6) and sCMOS ORCA-Flash4.0 V2 camera (Hamamatsu)). In a separate experiment, VinTS MSCs were seeded as described above, allowed to attach and spread overnight, then TRPV4 was activated via GSK101 (10 nM for 30 minutes) and cells were fixed either immediately or allowed to recover (4h, 24h, 48h), with FRET images obtained immediately following fixation.

Image analysis was performed using custom written code in MATLAB (Mathworks). FRET was detected through measurement of sensitized emission and calculated on a pixel-by-pixel basis as described previously (6). Briefly, images were first corrected for uneven illumination, registered, and background-subtracted. Spectral bleed-through coefficients were determined and corrected for as described in (6), and FRET efficiencies were calculated using the proportionality method described in (8). For all FRET images, focal adhesions (FAs) were identified in the acceptor channel and segmented using the water algorithm (9). Each identified adhesion was considered as a single unit and average FRET efficiency for each FA was calculated.

Statistical Methods. Unless otherwise noted, all data is presented as mean and standard error, and corrected for multiple comparisons where appropriate. For calcium signaling analyses, differences in percentage of cells signaling during the image acquisition period were assessed via Pearson's chi-squared analysis. Bar plots for this metric are presented without error bars as this measure is binary (cells do/do not signal during the observation time) and bars represent the percentage for the entire experimental condition, group, or time point (50-150 cells/condition, specific numbers listed in figure captions). Differences in the time between signal peaks were determined via Kruskal-Wallis test and Dunn post hoc analysis. Differences in polarized light intensity were tested via ANOVA with Dunnett's post hoc analysis. FRET efficiency and focal adhesion size were assessed via ANOVA with Tukey HSD post hoc test (for inhibition experiments, Fig.3C) or Dunnett's post hoc test (activation experiments, Fig.3D). Differences in cell nuclei alignment were assessed by binning alignment angle data (15° bins, $-90° < \theta < 90°$), with comparison of distributions made via Kolmogorov-Smirnov test ($\alpha < 0.05$ significant).

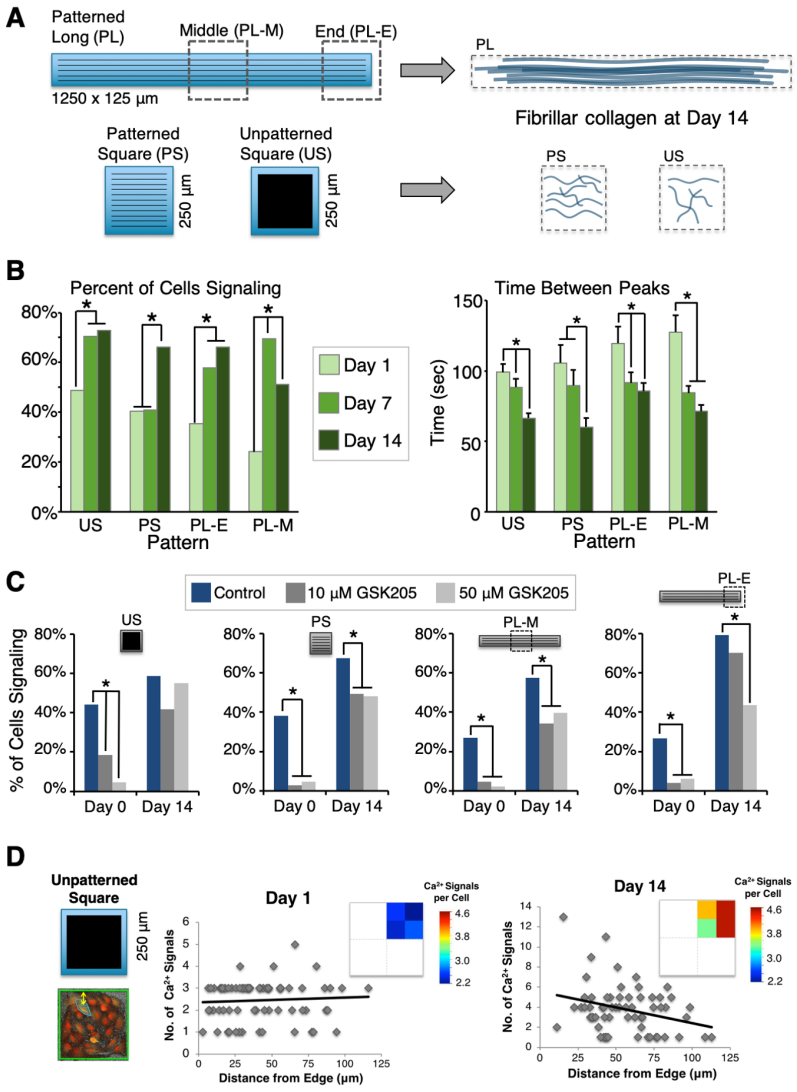

Figure S1. MSC Ca^{2+} signaling behavior is insensitive to pattern microenvironment, developing collagen matrix, and sub-pattern spatial position. (A) MSCs cultured on micro-photopatterns (µPPs) with varying micro-scale cell-adhesive architectures (patterned, unpatterned) and macro-scale boundaries (square, long) produce high (pattern type PL) or low (pattern types PS, US) amounts of aligned fibrillar collagen (right, as previously described in (1)). (B) With culture time, the percentage of MSCs signaling increases (left, bars represent percentage of cells signaling for the entire population/condition and thus do not have error bars) and time between signals decreases (right). *significant difference by chi-squared (% cells signaling) or Kruskal-Wallis (time between peaks), $p<0.05$, n=58-148 cells/condition/time point. (C) Blocking TRPV4 activity reduces Ca^{2+} signaling in a similar manner across all pattern types. *significant difference by chi-squared, $p<0.05$, n=63-150 cells/condition/time point. (Note: PL-E data is repeated here from Fig.2D for ease of comparison.) (D) To assess whether Ca^{2+} signaling varied with cell spatial position within patterns, the minimum distance from a cells's centroid to the pattern edge was plotted versus signaling frequency (number of peaks). At Day 1, no relationship was detected ($p=0.58$, $R^2 = 0.004$). At Day 14, a significant correlation was observed on unpatterned square (US) patterns, with cells near the edge signaling with greater frequency ($p=0.022$, $R^2 = 0.085$). Other pattern configurations (PS, PL) did not show significant correlations at any time point.

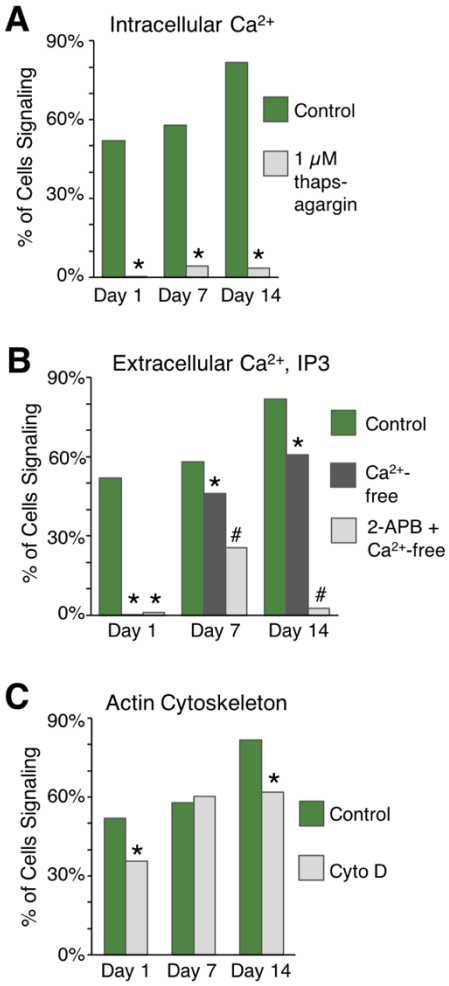

Figure S2. Ca^{2+} signaling at later times does not require external Ca^{2+}, involves IP3-mediated internal Ca^{2+} store release, and is insensitive to actin cytoskeletal disruption. (A) Ca^{2+} signaling in MSCs cultured on μPPs (signaling in PL-E pattern region shown, bars represent percentage of cells signaling for the entire cell population/condition and thus do not have error bars) was completely inhibited when intracellular stores were depleted via thapsagargin treatment (*$p<0.05$). (B) Early (Day 1), MSC Ca^{2+} signaling required the presence of external Ca^{2+}, but at later times (Days 7, 14) removing extracellular Ca^{2+} had less effect (*different from control, chi-squared, $p<0.05$). Adding IP3 receptor antagonist 2-APB further decreased signaling (# different from Ca^{2+}-free, chi-squared, $p<0.05$). (C) Disrupting the actin cytoskeleton via cytochalasin D (2 mM) had only a mild effect on Ca^{2+} signaling. n = 56-202 cells/condition/time point.

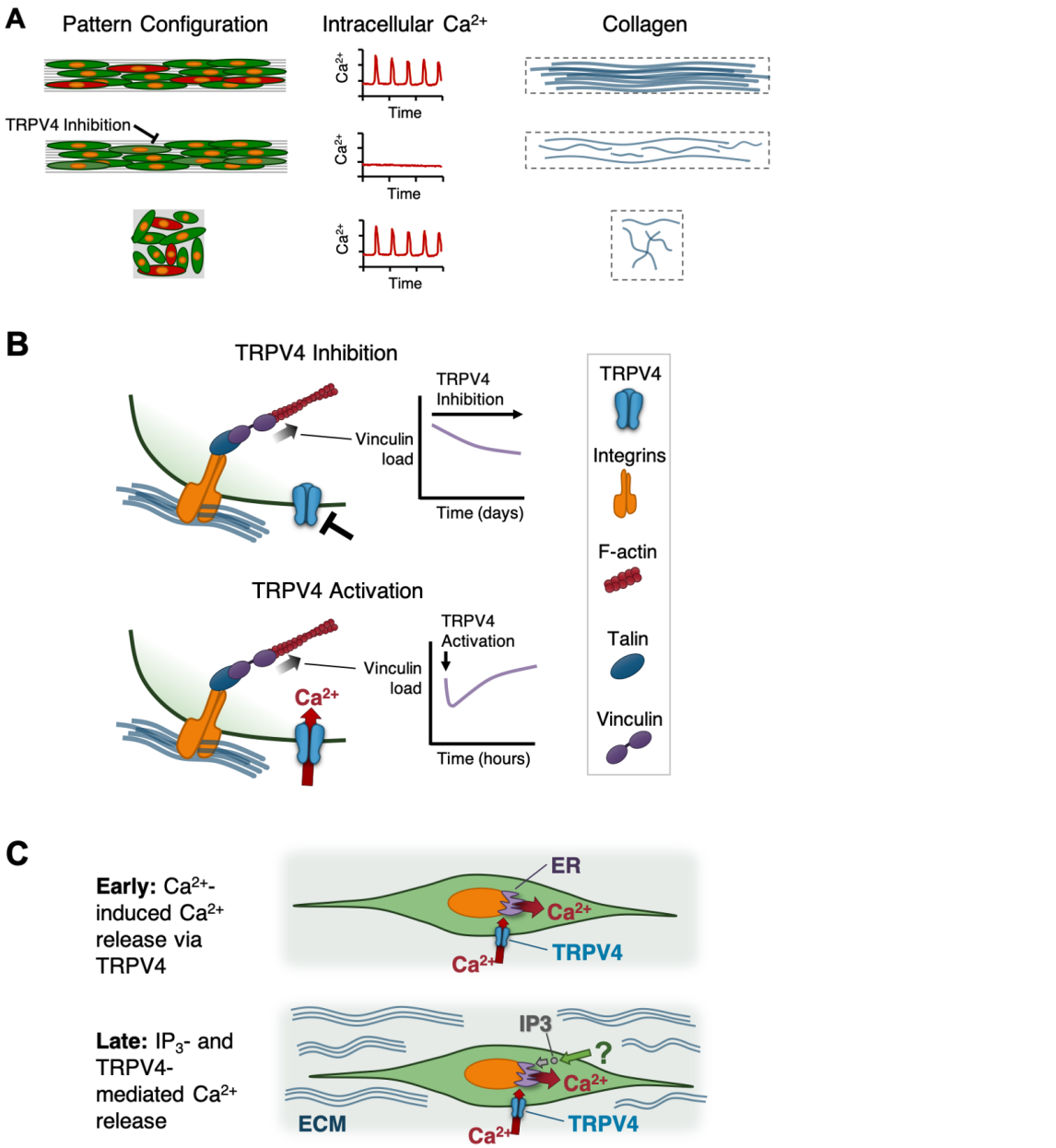

Figure S3. Summary of MSC Ca^{2+} signaling during aligned collagen matrix formation. (A) MSCs cultured on micropatterns that force multicellular alignment and end-to-end cell positioning (top, >~500 μm pattern length (1)) exhibit oscillating Ca^{2+} signaling and assemble aligned fibrillar collagen. Blocking TRPV4 (center) disrupts Ca^{2+} signaling and inhibits aligned collagen formation. When cultured on micropatterns that do not promote cell alignment (bottom), MSCs exhibit similar Ca^{2+} signaling behaviors but fail to assemble fibrillar collagen. Together, this suggests MSC TRPV4-dependent oscillating Ca^{2+} signaling is insensitive to pattern microenvironment and is necessary for aligned collagen formation, but not sufficient in the absence of appropriate physical (microarchitectural) cues. (B) When TRPV4 activity is continuously inhibited, tensile load across vinculin is decreased over the course of days. A stimulus activating TRPV4 results in a rapid (minutes) decrease, followed by recovery (hours), of tensile load across vinculin. (C) Early in aligned collagen development, TRPV4 mediates Ca^{2+} release from intracellular stores such as the endoplasmic reticulum (ER). Later in matrix development, extracellular Ca^{2+}-independent, inositol triphosphate (IP3)-mediated intracellular calcium store release contributes significantly to signaling.

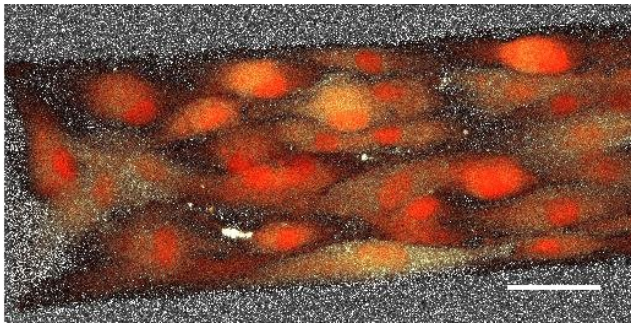

Movie S1. MSCs cultured on μPP substrates exhibit oscillating calcium signaling during aligned collagen matrix formation. Ratiometric calcium imaging of MSCs on patterned long (PL) μPP substrates following 1 day of culture. Movie captures 5 minutes of signaling, with imaging at 1.8 second intervals (movie frame rate = 10 fps, scale bar = 50 μm).

References

1. Gilchrist CL, Ruch DS, Little D, & Guilak F (2014) Micro-scale and meso-scale architectural cues cooperate and compete to direct aligned tissue formation. *Biomaterials* 35(38):10015-10024.
2. Doyle AD, Wang FW, Matsumoto K, & Yamada KM (2009) One-dimensional topography underlies three-dimensional fibrillar cell migration. *J Cell Biol* 184(4):481-490.
3. Tian W*, et al.* (2004) Renal expression of osmotically responsive cation channel TRPV4 is restricted to water-impermeant nephron segments. *Am J Physiol Renal Physiol* 287(1):F17-24.
4. Phan MN*, et al.* (2009) Functional characterization of TRPV4 as an osmotically sensitive ion channel in porcine articular chondrocytes. *Arthritis Rheum* 60(10):3028-3037.
5. Grashoff C*, et al.* (2010) Measuring mechanical tension across vinculin reveals regulation of focal adhesion dynamics. *Nature* 466(7303):263-266.
6. Rothenberg KE, Neibart SS, LaCroix AS, & Hoffman BD (2015) Controlling Cell Geometry Affects the Spatial Distribution of Load Across Vinculin. *Cell Mol Bioeng* 8(3):364-382.
7. Rothenberg KE, Scott DW, Christoforou N, & Hoffman BD (2018) Vinculin Force-Sensitive Dynamics at Focal Adhesions Enable Effective Directed Cell Migration. *Biophys J* 114(7):1680-1694.
8. Chen H, Puhl HL, 3rd, Koushik SV, Vogel SS, & Ikeda SR (2006) Measurement of FRET efficiency and ratio of donor to acceptor concentration in living cells. *Biophys J* 91(5):L39-41.
9. Zamir E*, et al.* (1999) Molecular diversity of cell-matrix adhesions. *J Cell Sci* 112 (Pt 11):1655-1669.